Organic/polymeric electroluminescent devices processed by hybrid ink-jet printing

YANG YANG, SHUN-CHI CHANG, JAYESH BHARATHAN, JIE LIU
Department of Materials Science and Engineering, University of California, Los Angeles, CA 90095, USA
E-mail: yy@seas.ucla.edu

Ink-jet printing (IJP) technology is a popular technology for desktop publishing. Since some of the conducting (or conjugated) organic molecules and polymers are solution processable, IJP becomes an ideal method for printing polymer/organic light-emitting diodes with high resolution. In this review article, we present the hybrid ink-jet printing technology (HIJP), which consists of an ink-jet printed layer in conjunction with another uniform spin-coated polymer layer, which serves as a buffer layer to seal the pin holes between the ink droplets. This HIJP technology has been successfully applied to the fabrication of polymer light-emitting logos, multicolor polymer/organic light-emitting diodes, and the built-in shadow mask for the cathode patterning for pixelated polymer LEDs.

1. Introduction

Polymer light-emitting diodes (PLEDs) and organic light-emitting diodes (OLEDs) have a potential for extensive applications such as multicolor emissive displays, road signs, indicator lights, and logos [1–3]. One of the major advantages of PLEDs and OLEDs is their color tuning capability with various emission colors easily obtained through the change of chemical structure of the organic compounds. Another advantage is the solution processability of the conjugated organics [4]. Traditionally, the polymer solutions are deposited by spin-coating; a technology incapable of patterning materials, since it non-selectively distributes the materials all over the substrate. However, to realize the above-mentioned applications, such as multicolor displays, it is necessary to achieve a lateral control during deposition of the different polymers such that multicolor emission can be achieved. This drawback of spin-coating can be overcome by using the ink-jet printing (IJP) technology. IJP technology is a common technology used for desktop publishing. It is a contactless method of printing and has found wide applications in the packaging and printing industries. Ink-jet printers work on the principle of ejecting a fine jet of ink through nozzles 10–200 μm in diameter. The jetted stream is broken up into a series of droplets that are deposited as a dot matrix image. The advantages of the ink-jet printing technology over the conventionally used spin-coating technology are shown in Table I.

2. Hybrid ink-jet printing (HIJP)

Although IJP is ideal for printing polymer and organic solutions, this technology cannot be used in its original form. This is due to the unavoidable presence of voids between the solution droplets, leading to electrical shorting points in the regions where the cathode and anode metals contact each other. This can be clearly understood from Fig. 1. To overcome these drawbacks and successfully apply the patterning capability of the ink-jet printing technology, we here at UCLA developed the hybrid ink-jet printing technology (HIJP) [5].

This technology consists of an ink-jet printed layer in conjunction with another uniform, spin-coated (or precision-coated) polymer layer. This uniform layer which is called the buffer layer, serves to seal the pin holes while the ink-jet printed layer consists of the desired pattern, for example the red-green-blue dots for a multicolor display. The use of the polymer buffer layer is demonstrated in Fig. 1. Below is a brief description of the unique characteristics of the HIJP technology:

- The buffer layer is a pin-hole-free layer which can seal the pin holes produced by the ink-jet printed layer.
- The buffer layer could be the ink absorbing layer and could effectively ''fix'' the printed materials when a proper solvent for the ink has been chosen. In addition, this buffer layer effectively planarizes the surface roughness produced by the ink-jet printed dots.
- Due to the small diameter of the jet nozzle, and the high molecular weight of the conjugated polymer, IJP is ideal for printing small amounts of materials. Therefore, this technology is ideal for the deposition of dopants. Multicolor emission can be realized from an efficient energy transfer, when the buffer layer is a wide bandgap semiconducting polymer layer, and the ink-jet printed materials are the dopants with smaller bandgaps than the buffer layer.

TABLE I Comparison of spin-casting and ink-jet printing technologies

Characteristics	Spin-casting	Ink-jet printing
Patterning capability	No patterning capability	Capable of patterning with micrometer resolution
Large device area capability	Sensitive to dust particles and substrate defects, and not suitable for large area processing.	Not sensitive to substrate defects, and it is a better technology for the fabrication of large area device.
Efficiency of using material	More than 99% of the polymer solution is wasted.	Less than 2% of the material is wasted.
Multicolor display fabrication capability	No multicolor patterning capability.	Ideal for multicolor patterning.

The HIJP concept is a unique approach for fabricating polymer and organic electronic devices. One is able to apply this technology for the deposition of various functional materials such as charge-injection layers, charge-blocking layers, and multicolor polymer/organic emissive layers. We have demonstrated all of these possibilities by making four different types of devices: polymer light-emitting logos, dual-color PLEDs, multi-color OLEDs, and pixelated PLEDs. These four devices and the ink-jet printed materials are listed in Table 2. The discussion of these four devices is the main focus of this review article.

3. Polymer light-emitting logo

The first example of the successful application of HIJP technology is the polymer light-emitting logo [3]. In this example, we used a water-soluble conducting polymer PEDOT (3,4-polyethylenedioxythiophene-polystyrene-sulfonate) as the ink for the printer and used an emissive polymer MEH-PPV as the buffer layer. To fabricate the polymer light-emitting logos (PLELs) we printed the desired pattern on the glass/ITO substrates measuring $3 \, cm \times 3 \, cm$ followed by spin-coating of the emissive polymer MEH-PPV. Typical thickness of the film was around 100 nm as determined by Alpha-step profilometry. The devices were then fabricated in air by routine LED technology. The fabrication procedure is schematically shown in Fig. 2.

Since the charge injection efficiency of conducting polymer is much better than that of ITO, only the areas covered by the conducting polymer illuminate under the same operating voltage [6]. Therefore the ink-jet printed PEDOT defines the pattern of the logo. The voltage–brightness measurements in Fig. 3 show significant difference in performance between these two types of devices. For example, when the device is operated at 5 V, the ITO/PEDOT/MEH-PPV/Ca device has around $200 \, cd \, m^{-2}$ brightness while the brightness from the ITO/MEH-PPV/Ca device was about three orders of magnitude smaller. This gives a contrast, defined as the brightness ratio of the bright/dark regions, of approximately 800.

Fig. 4 illustrate a polymer light-emitting UCLA logo and a valentine hearts logo demonstrated by this technology. Since images from a personal computer can be directly printed to form the light-emitting logo this technology has very broad applications. For instance, new and complicated emissive logos can be custom-built for a variety of purposes such as greeting cards or other novelty items.

One can easily extend this concept of light-emitting logos to light-emitting pictures. However, one of the major concerns of applying this technology in achieving high quality light-emitting pictures is the gray scale.

In Fig. 5a, we demonstrate a four-level gray scale generated from a computer graphic program. The density of emissive dots defines the gray scale and Fig. 5b shows

TABLE 2

Devices fabricated	IJP material	Buffer material
Polymer light-emitting logo	Hole-injection layer: PEDOT[a]	EL polymer: MEH-PPV[b]
Dual-color PLED	Red-emission polymer: MPS-PPV (Diffusion of MPS-PPV into PPP buffer layer, energy transfer occurred)	Blue-emission polymer: PPP-NEt₃[c]
Multicolor OLED	Green emission organic molecule: Almq₃ Red-emission organic dye: DCM (Bilayer structure, no diffusion occurred)	Blue-emission polymer: PVK[d]
Pixelated PLED	Insulating polymer: PVA[e] is used as the insulating shadow mask for the patterning of cathode.	EL polymer: MEH-PPV

[a]PEDOT (3,4-polyethylenedioxythiophene-polystyrenesulfonate) [b]MEH-PPV: Poly(2-methoxy-5-(2′-ethyl-hexyloxy)-1,4-phenylene vinylene) [c]PPP-NEt₃⁺: poly[2,5-bis[2-(N,N,N-triethylammonium) ethoxy]-1,4-phenylene-alt-1,4-phenylene] dibromide [d]PVK: poly-9-vinylcarbazole [e]PVA: polyvinylalcohol
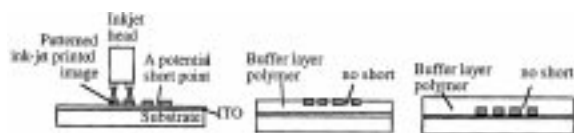
Figure 1 IJP technology in its original form; left. The combination of IJP technology and a buffer layer (the HIJP technology); middle and right. Middle; the buffer layer can be the bottom polymer layer which absorbs the IJP droplets. Left; the buffer layer can be above the IJP layer and seal the pin holes.
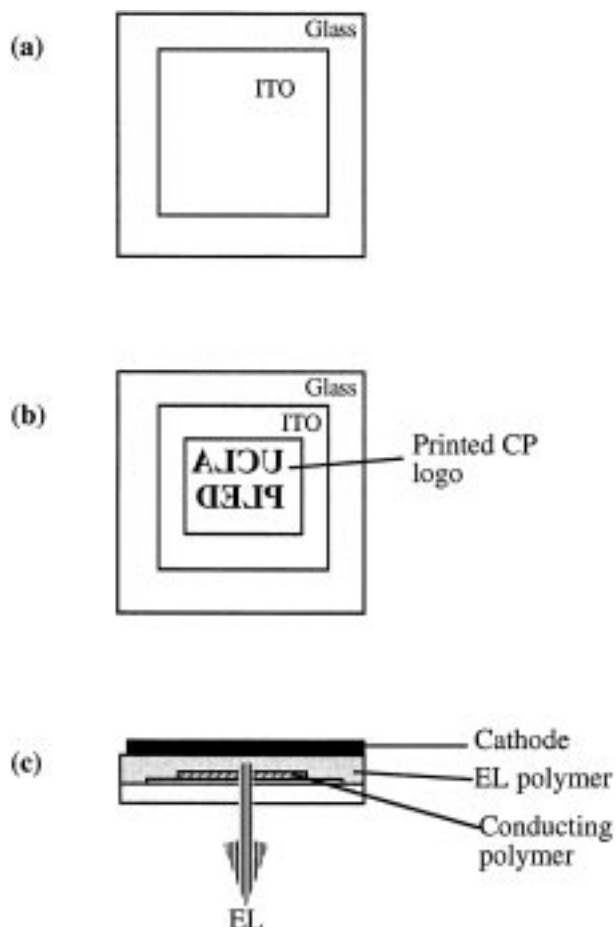

Figure 2 The polymer light-emitting logo fabrication process; (a) preparation of the substrate, (b) printing of the conducting polymer into the desired pattern, and (c) deposition of the luminescent polymer and the cathode material.
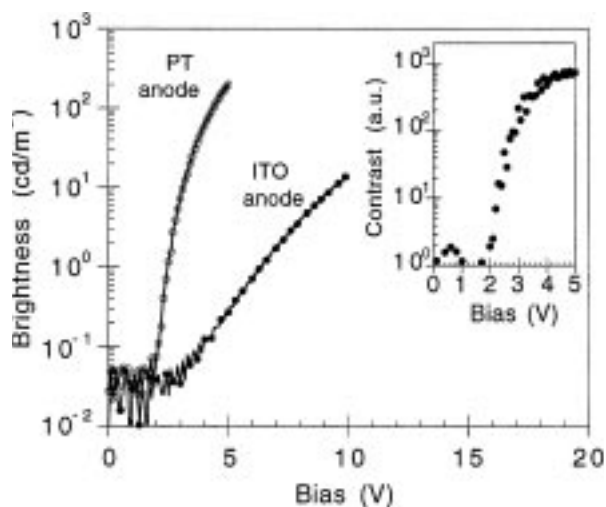

Figure 3 The brightness–voltage curves of the devices with and without PEDOT as the hole injection layer. The contrast–voltage curve is shown in the inset.

the brightness of each level of gray scale. This gray scale can be tuned nearly continuously by changing either the dot size or the density of dots. Another advantage of this ink-jet printing technology is the fabrication of micro-meter-sized polymer light-emitting diodes without going through the regular patterning of anode and cathode. Usually, small-sized LEDs can only be fabricated by crossing the cathode and anode fingers with the overlap area defining the pixel size. This unique pattering capability of the ink-jet printer using the conducting polymer provides a convenient alternative for the generation of regular arrays of micrometer-sized polymer LEDs. Typical emissive dot sizes mentioned in this report ranged from $180\,\mu m$ to $400\,\mu m$ depending on the amount of conducting polymer ink sprayed from the nozzle. The dimensions of the pixels produced by this technology are also a function of the nozzle size of the ink-jet head and it can be reduced if the nozzle size is reduced.

4. Dual-color polymer light-emitting diodes
The most promising application of ink-jet printing is the fabrication of polymer multicolor displays. Hence, the second example to illustrate the potential of the HIJP technology is the fabrication of a dual-color PLEDs [7]. To fabricate dual-color pixels, the polymer buffer layer used was a wide-bandgap, blue-emitting semiconducting polymer, poly[2,5-bis[2-(N,N,N-triethylammonium) ethoxy]-1,4-phenylene-alt-1,4-phenylene] dibromide $(PPP-NEt_3^+)$, prepared by the spin-casting technique and was approximately 200 nm thick as determined by profilometry. The ink-jet printed layer was a red-orange semiconducting polymer, poly(5-methoxy-2-propanoxy-sulfonide-1,4-phenylene vinylene) (MPS-PPV) which was printed onto the buffer layer. A thin layer of conducting polymer, polyaniline, was spin-coated onto the ITO as an efficient hole-injection layer [6]. The $PPP-NEt_3^+$ solution was prepared in acidic DI water $(pH = 4)$ at $1\,wt\%$ concentration, and the MPS-PPV solution was prepared in neutral DI water at $2\,wt\%$ concentration.

The $PPP-NEt_3^+$ buffer layer plays a critical role in this dual-color device. The $PPP-NEt_3^+$ is first synthesized as a neutral polymer that is soluble in organic solvents $(CHCl_3, THF)$ and in acidic water through quaternization of the amine functionality. In a second step, the neutral polymer is subject to treatment with bromoethane to yield the bromide salt of the polymer. This form of the polymer has varying neutral water $(pH = 7)$ solubility characteristics depending on the number of amine sites quaternized. This particular $PPP-NEt_3^+$ sample was quaternized such that an aqueous solution of $pH = 4$ was necessary to achieve the desired solubility. This unique property makes $PPP-NEt_3^+$ an ideal ink absorbing material for the MPS-PPV, which was prepared in neutral DI water. If the $PPP-NEt_3^+$ were completely soluble in

Figure 4 The polymer light emitting logo patterned by the IJP technology; (a) a UCLA logo, and (b) a valentine hearts logo.
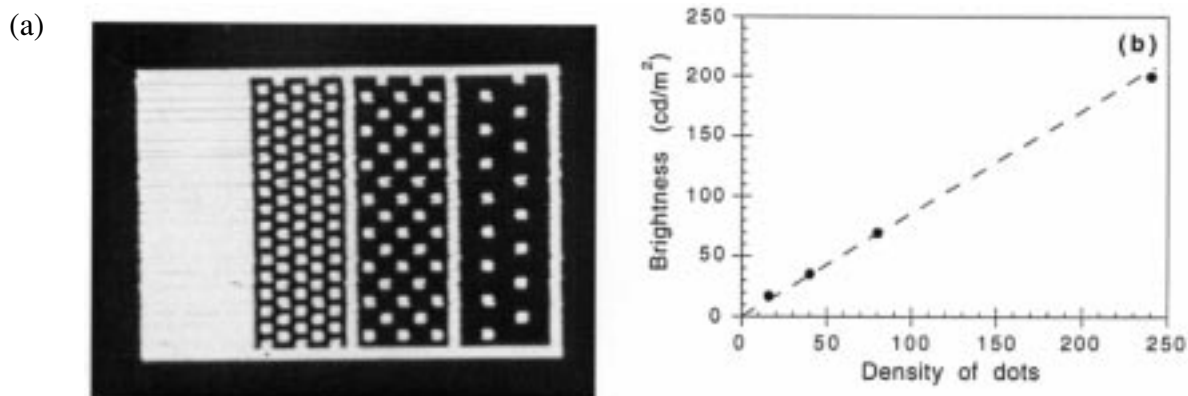

Figure 5 (a) Four levels of gray scale of the polymer light-emitting logo created by ink-jet printing technology (the brightness of these four regions is defined by the density of dots), and (b) brightness versus density of dots.

the neutral DI water, then the solvent of MPS-PPV would have smeared the buffer layer. Hence, the concepts of ink absorbing (or dopant diffusion) and the energy transfer effect are successfully demonstrated in this PPP-NEt$_3^+$:MPS-PPV system. The solvent of the ink-jet printed MPS-PPV slightly dissolves the PPP-NEt$_3^+$ layer and allows the MPS-PPV to diffuse into the PPP-NEt$_3^+$ layer. This leads to an efficient energy transfer from the PPP-NEt$_3^+$ to the MPS-PPV, thereby generating a red-orange photoluminescence and electroluminescence from the ink-jet printed sites. Based on this

principle, blue and orange-red dual-color polymer light-emitting diodes were fabricated on the same substrate.

Four LEDs were fabricated on one substrate. Two were blue emission LEDs (devices A and B), and the other two were orange-red emission devices (devices C and D), as can be seen from Fig. 6. The PL and EL spectra were measured using an Ocean Optics Spectrometer.

The photoluminescent (PL) spectrum of the PPP-NEt$_3^+$:MPS-PPV blend is identical to the MPS-PPV PL spectrum, and this is direct evidence of the
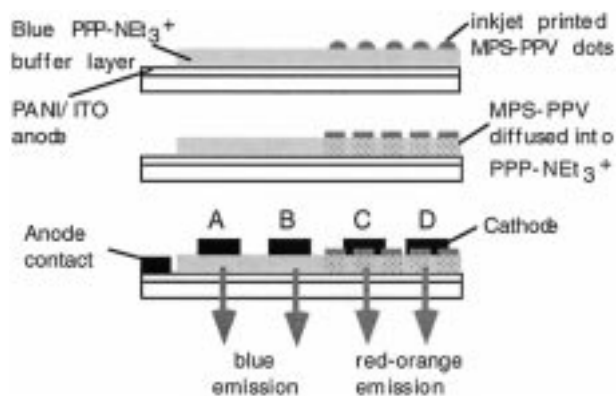

Figure 6 The device structure of dual-color polymer light-emitting diodes. Devices A and B are blue emitting LEDs with PPP-NEt$_3^+$ as the active material. Devices C and D are red-orange devices with PPP-NEt$_3^+$: MPS-PPV as the active material.
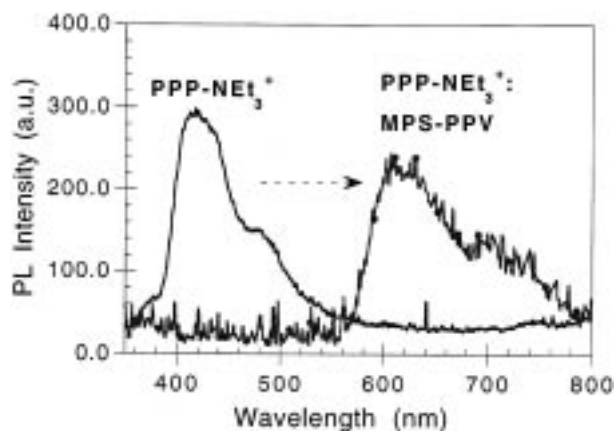

Figure 7 The PL emission of the PPP-NEt$_3^+$ and PPP:MPS-PPV. EL spectra are similar. There is no blue emission in the PPP-NEt$_3^+$. MPS-PPV blend and this spectrum indicates that the energy has been transferred from PPP-NEt$_3^+$ to MPS-PPV.
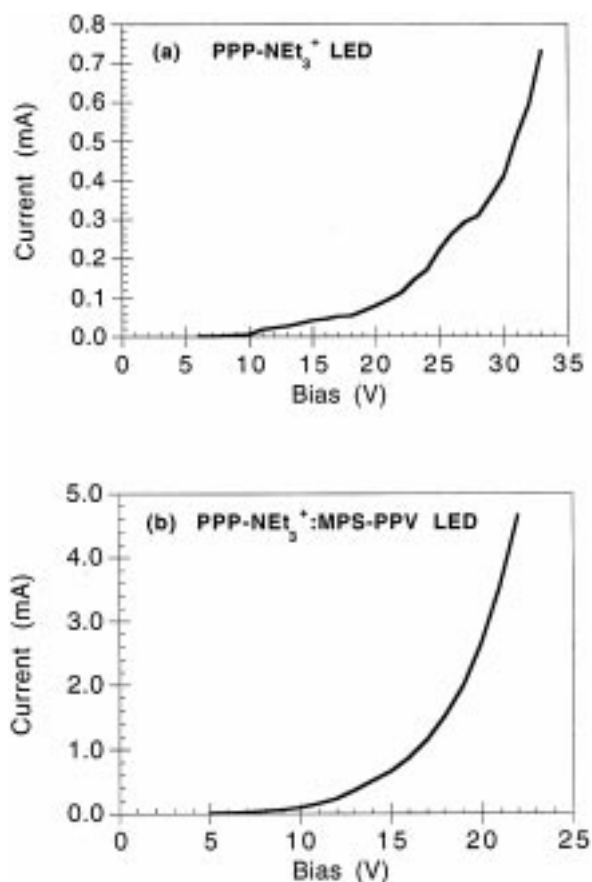
Figure 8 The *I–V* curves of the two types of devices; (a) ITO/PANI/ PPP-NEt$_3^+$/Ca, and ITO/PANI/PPP-NEt$_3^+$:MPS-PPV/Ca. The device area is about 0.1 cm^2.

dopant diffusion and energy transfer effects discussed earlier. The PL spectra of PPP-NEt$_3^+$ and PPP-NEt$_3^+$:MPS-PPV are shown in Fig. 7. The current–voltage curves of the PPP-NEt$_3^+$ and PPP-NEt$_3^+$:MPS-PPV devices are shown in Fig. 8. The slightly high operating voltage for both types of LEDs was due to the thick PPP-NEt$_3^+$ layer. The PPP-NEt$_3^+$:MPS-PPV system has a much lower turn-on and operating voltage than that of the PPP-NEt$_3^+$ system. This may be due to the fact that MPS-PPV has a smaller bandgap and hence carrier injection and carrier transport is much easier than that of the PPP-NEt$_3^+$ system. The brightness of both devices is, however, not very high. For the blue emission, the peak brightness at 33 V was about 10 cd m^{-2}. For the red emission, the peak brightness at 22 V was about 7 cd m^{-2}. The reason for such low brightness is probably due to the fact the devices were fabricated in air and photochemical oxidation reaction could have damaged the polymer. In addition, the low efficiency and brightness of the device could also be due to the usage of DI water and acidic DI water as the solvents for the MPS-PPV and PPP-NEt$_3^+$, respectively.

These examples, the blue- and red-emitting PLEDs, indicate that the choice of the solvent used for the IJP material (the dopant) is very important in achieving the dopant diffusion and energy transfer effect. These two examples also illustrate the advantage of the HIJP technology in controlling the local morphology between the dopant and the buffer layer (the host). The details of the diffusion process, the local morphology, and the

potential of forming high surface area contact between the dopant polymer and the host polymer are still under investigation.

5. Multicolor organic light-emitting diodes

The third example we demonstrated was multicolor organic light-emitting diodes (OLEDs). In addition to polymer light-emitting diodes, HIJP can also be applied to the OLEDs [8]. The traditional fabrication of OLED involves the thermal sublimation of organic materials in an ultra-high vacuum environment. However, this process is rather time-consuming and complicated for patterning fine multicolor pixels. As illustrated earlier, HIJP allows a convenient alternative for the patterning of multicolor pixels through an efficient energy transfer from an appropriate buffer layer (a semiconducting polymer layer) with a wide bandgap to the ink-jet printed materials (dopants) with smaller bandgaps than the buffer layer. Alternatively, the buffer layer can be continuous polymer layer insoluble in the solvents used by the IJP droplets. In this case, it seals the pin holes and can also function as the hole-transport layer (HTL). The latter case is ideal for the fabrication of organic LEDs, since the most efficient OLEDs comprise a bilayer structure of a HTL and an emissive layer [9].

To fabricate organic multicolor LEDs by this technology we used a blue-emitting, semiconducting polymer, poly-9-vinylcarbazole (PVK) as the buffer layer. This layer was approximately 150 nm thick. The ink-jet printed dopants used were tris(4-methyl-8-quinolinolato)Al (III) (Almq$_3$) [10] and DCM (4-(dicyanomethylene)-2-methyl-6-(4-dimethyl aminostyryl)-4H-pyran), which were printed on the PVK buffer layer. Based on this principle, multicolor organic LEDs comprising of bilayer structures of PVK/DCM (orange-red emission), PVK/Almq$_3$ (green-blue emission) were fabricated with the blue emission PVK buffer layer serving as the hole-transport layer.

Due to the inability of the commercially available ink-jet printer to resist the corrosive action of regular solvents, methanol was chosen as the solvent for DCM and Almq$_3$, with each dopant deposited separately. The device structure of the ink-jet printed multicolor organic LEDs is similar to the device shown in Fig. 6. Each substrate consisted of four LEDs, two of which were blue-emission LEDs (devices A and B in Fig. 6) with PVK as the active material. The remaining two were either orange-red or blue-green emitting LEDs (devices C and D in the same figure) with the emission obtained from the PVK/DCM or PVK/Almq$_3$ bilayer structures, respectively. A thin layer of PEDOT was spin-coated onto the ITO for efficient hole injection and PVK was chosen as the buffer layer because of its insolubility in methanol. Hence, a well defined bilayer structure can be obtained by using this layer.

For the orange-red emissive devices, DCM was printed onto the PVK layer whereas for the green-emission device, Almq$_3$ was printed onto the PVK buffer layers using the same printer. The spin-coating of PVK and the ink-jet printing process of DCM and Almq$_3$ was carried out in air. The volatile nature of methanol permits the localized deposition of the Almq$_3$ and DCM droplets and
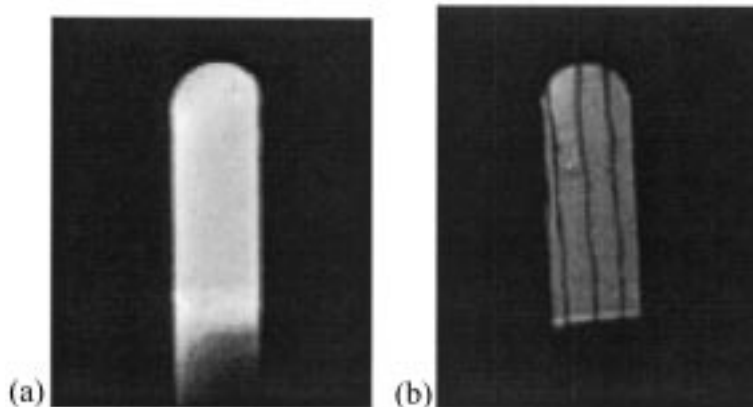
Figure 9 Pictures of an OLED with Almq$_3$ as the emission material. In (a) Almq$_3$ is processed by the thermal sublimation process and in (b) Almq$_3$ is process by ink-jet printing.

hence no smearing of these droplets occurred on printing. For the purpose of comparison, a regular organic LED with the structure ITO/PEDOT/PVK/Almq$_3$/Ca was also prepared, with Almq$_3$ deposited by vacuum sublimation.

Fig. 9 shows the pictures of the Almq$_3$-based LEDs fabricated by the thermal deposition and the HIJP processes. These two pictures were taken under identical conditions of exposure and the results qualitatively reflect the difference in the emission intensities between these two devices. The device fabricated by thermal sublimation shows more uniform emission than the ink-jet printed device. The thin dark lines seen crossing devices fabricated by the HIJP are caused by some clogged nozzles in the printer head that resulted in no material being printed along these lines. This is a common problem afflicting ink-jet printers and hence demonstrates the importance of the buffer layer. Without the buffer layer it would be virtually impossible to make good devices due to the unavoidable presence of pin holes that are associated with the IJP technique.

The current–voltage (*I–V*) and light–voltage curves (*L–V*) for the PVK/Almq$_3$ bilayer LEDs fabricated by the HIJP are shown in Fig. 10a, and the PL and EL emission spectra are shown in Fig. 10b. The device turned-on at around 8 V and the external quantum efficiency was about 0.02%. On the other hand, the devices obtained by the thermal sublimation process were superior to their ink-jet printed counterparts. The device efficiency was about 10 times higher (0.2%) with a much better device stability. One of the reasons for the low efficiency and short lifetime for the LEDs fabricated using the HIJP technology could be due to the fact that since the devices were fabricated in air, significant device degradation could have occurred due to the presence of residual moisture and oxygen. Another possibility of the faster decay of the ink-jet printed devices is the difference in the morphology of Almq$_3$. Thermal sublimation results in films which are much more uniform than the ink-jet printed films. The PL and EL emission spectra from the devices with the ink-jet printed Almq$_3$ are identical to the spectrum obtained from an Almq$_3$ thin film deposited by thermal sublimation. This is an indication that the recombination zone is entirely within the Almq$_3$ layer and that the PVK layer functions only as the hole-transport layer. However, the small peak in the EL

spectra around 600 nm is perhaps due to the molecular aggregation of Almq$_3$ [11]. The peaks at 370 nm and 740 nm in the PL spectrum are from the mercury lamp source, which was used for the PL measurements.

Fig. 11 shows the color pictures of red-green-blue LEDs. The red-emission device, with DCM as the emissive material, has an emission spectrum consistent with regular DCM. (The QE was estimated to be less than 0.01%.) Analogous to the PVK/Almq$_3$ bilayer structure, this is an indication that the recombination zone is entirely within the DCM layer and that PVK functions as the hole-transport layer. The blue devices, with the structure of ITO/PEDOT/PVK/Ca, exhibit a blue-purple color. In this device structure, the PVK layer behaves as the active layer for generation of electroluminescence.
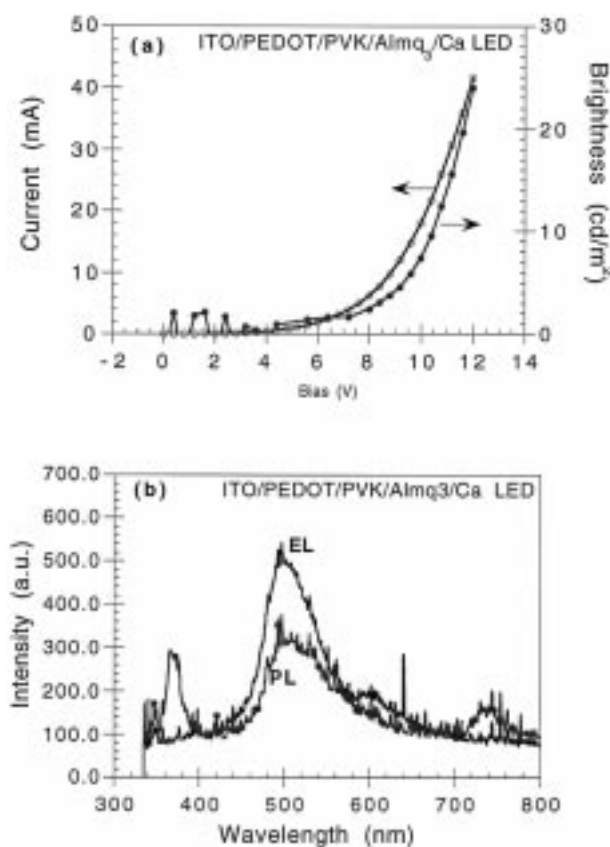

Figure 10 (a) The current–light–voltage (*I–L–V*) curves, and (b) EL and PL emission spectra for the ITO/PEDOT/PVK/Almq$_3$ LED.
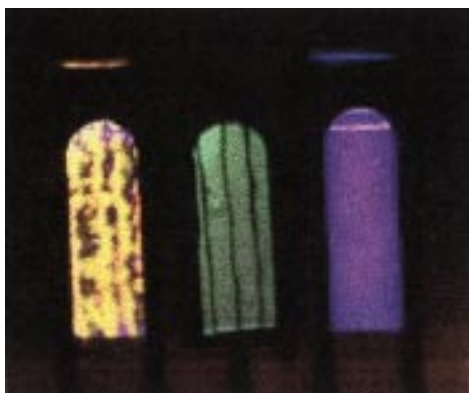
94

Figure 11 Color pictures of red, green and blue OLEDs. The red and blue LEDs are on the same substrate and the green LED was fabricated on a separated substrate.

However, there is a red emission peak in the spectrum of PVK. This phenomenon has been previously observed and has been attributed to the defects in the PVK film or perhaps due to the moisture absorbed during the spin-casting process and the ink-jet printing processes, which were carried out in air [12].

6. Shadow mask by ink-jet printing

Our final example of the HIJP technology is the demonstration of shadow mask for the patterning of cathode metal. In addition to the multicolor patterning capability, another important technical issue for the EL display is the patterning of the anode and the cathode. For the organic EL displays, the earliest and lowest cost way of driving the display is the so-called ''X-Y'' passive addressable driving scheme, achieved through the patterning of the anode and the cathode materials into mutually perpendicular row and column electrodes. The patterning of ITO is achieved by regular photolitho-graphy with high resolution. On the other hand the patterning of the cathode is somewhat difficult. The photolithography process cannot be applied to pattern the cathode, since the solvents that process the photoresist would destroy the underlying organic materials. Therefore, the cathode patterning is usually achieved by using stainless steel shadow masks. However, this technique lacks the required fine resolution. An alternative method could be the use of prepatterned mushroom-shaped photoresist dividers, on top of the active organic layers to serve as shadow masks. Apart from demonstrating the multicolor patterning capability, we also demonstrated the patterning of a ''built-in'' shadow mask though the ink-jet printing of inert polymers.

Fig. 12 shows the picture of patterned metal (cathode) strips using this technique. The printed material is an aqueous solution of polyvinylalcohol (PVA). As can be seen from the figure, the spacing between the ink-jet printed lines determines the width of the cathode. The width of the metal strip or the opening of the shadow mask that we have demonstrated is about 1 mm. Eventually the metal line width can be reduced to the resolution of the ink-jet printer, which has recently been improved, to 10 µm [13]. The thickness of the final PVA layer is estimated to be more than 1 µm. In the future, fabrication of shadow masks can be carried out after the printing of the multicolor organic compounds. This process will significantly simplify the procedure for fabricating organic multicolor, *X-Y* addressable passive matrix displays.

7. Conclusion

To summarize, we have demonstrated the feasibility of processing organic materials using the ink-jet printing technology. IJP is compatible with organic materials and
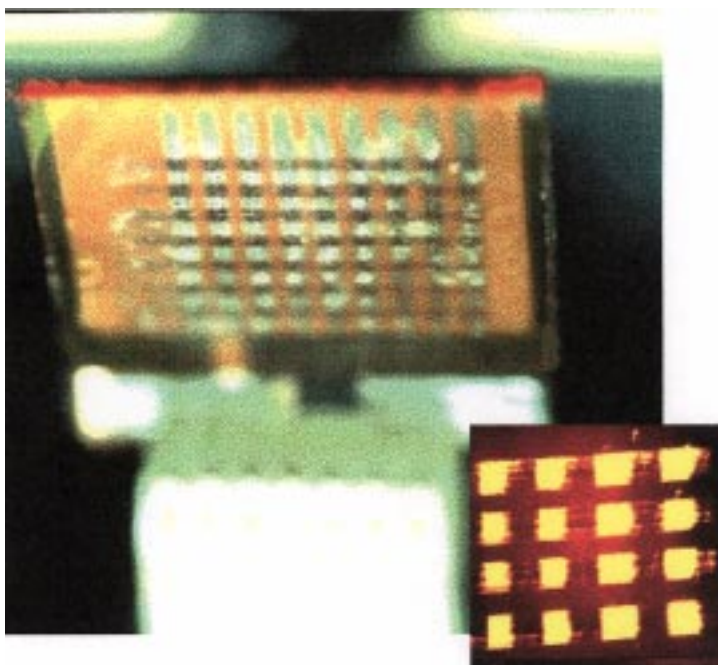

Figure 12 Column cathode (vertical shining metal strips) patterned by the ink-jet printed build-in shadow mask. Also shown is the row PEDOT anode (horizontal dark strips) printed directly by the IJP technology. The active polymer light-emitting pixels are shown as the inset.

also has other significant advantages such as being a low-cost technology and providing a convenient method for processing large area substrates. It is also environmentally friendly since there is minimal wastage of materials. This technology has tremendous advantages over the traditional spin-coating method of processing organic materials as can be seen from Table I. Since this technology is capable of addressing the critical issue of patterning organic materials its applications are unlimited. It can be used for the fabrication of logos, indicator lights, multicolor displays and also in bio-medical applications such as biosensors for low cost diagnostics.

Acknowledgment

References

1. J. H. BURROUGHES, D. D. C. BRADLEY, A. R. BROWN, R. N. MARKS, K. MACKAY, R. H. FRIEND, P. L. BURNS and A. B. HOLMES, *Nature* **347** (1990) 539; (b) G. GUSTAFSSON, Y. CAO, G. M. TREACY, F. KLAVETTER, N. COLANERI and A. J. HEEGER, *Nature* **357** (1992) 477.
2. H. NAKADA and T. TOHMA, ''Organic materials push EL displays into competition with LCDs'', Display Devices, Spring (no. 17) (1998) p. 29.
3. J. BHARATHAN and Y. YANG, *Appl. Phys. Lett.* **21** (1998) 2660.
4. D. BRAUN and A. J. HEEGER, *ibid.* **58** (1991) 1982.
5. (a) Y. YANG, US Patents Pending, Serial No. 60/062,294 and 60/072 709; (b) Y. YANG and J. BHARATHAN, *Proc. SPIE* **3279** (1998) 78.
6. Y. YANG and A. J. HEEGER, *Appl. Phys. Lett.* **60** (1994) 1245.
7. (a) S. C. CHANG, J. BHARATHAN, Y. YANG, R. HELGESON, F. WUDL, M. R. RAMEY and J. R. REYNOLDS, *ibid.* **73** (1998) 2561; (b) T. R. HEBNER and J. C. STURM, *ibid.* **73** (1998) 1775.
8. S. C. CHANG, J. LIU, J. BHARATHAN, Y. YANG, J. ONOHARA and J. KIDO, *Adv. Mater.* **11** (1999) 734.
9. C. W. TANG, S. A. VANSLYKE and C. H. CHEN, *J. Appl. Phys.* **65** (1989) 3610.
10. J. KIDO and J. Y. IIZUMI, *Appl. Phys. Lett.* **73** (1998) 2721.
11. FOTIS PAPADIMITRAPOLIS. Private communication.
12. (a) C. ZHANG, H. VON SEGGERN, K. PAKBAZ, B. KRAABEL, H.-W. SCHMIDT and A. J. HEEGER, *Synth. Met.* **62** (1994) 35; (b) C. ZHANG. Private communication.
13. G. PERCIN, T. S. LUNDGREN and B. T. KHURI-YAKUB, *Appl. Phys. Lett.* **73** (1998) 2375.